Human Telomere Quadruplex: Refolding and Selection of Individual Conformers via RNA/DNA Chimeric Editing†

Jianying Qi and Richard H. Shafer*

Department of Pharmaceutical Chemistry, School of Pharmacy, University of California, San Francisco, San Francisco, California 94143-0446

Received November 25, 2006; Revised Manuscript Received April 6, 2007

ABSTRACT: The conformation of the guanine quadruplex formed by the human telomere (HT) repeat in solutions containing physiological concentrations of K^+ ions has been a topic of intensive investigation during the past several years. Of particular interest are the directionality of the overall folding pattern, i.e., parallel, antiparallel, or a combination of these two modes, and the alternation, if any, of the glycosidic bond conformation between *syn* and *anti*. An additional issue involves resolving mixtures of conformations when more than one species is present. We approach these questions using selective substitution of riboguanosine, rG, for deoxyriboguanosine, dG. Using a combination of circular dichroism, gel electrophoresis, equilibrium ultracentrifugation, and imino proton NMR, we are able to show that these modifications can yield sequences which fold into parallel or antiparallel conformations consisting of one or two strands. We also demonstrate that chimeric editing of the HT sequence permits isolating one of two conformational isomers existing in solution in the presence of KCl. The ability to engineer and control quadruplex folding motifs illustrated here with HT may prove useful more generally for a variety of quadruplex-forming sequences.

Telomeres, the very end of linear chromosomes, contain a large number of guanine-rich repeats on one strand and terminate with a 3′ single-strand overhang involving this repeat (*1*). Guanine-rich repeats can readily fold on themselves, forming a unimolecular guanine quadruplex. These unusual nucleic acid structures require the presence of select mono- or divalent cations, representing a relatively unique example of specific metal ion complexation with nucleic acids via inner sphere coordination, as evidenced by both X-ray (*2*) and solution (*3*) studies. In the case of the *Oxytricha nova* telomere, formation of a quadruplex by the guanine-rich telomeric repeat has been shown to inhibit the activity of telomerase, the ribonucleoprotein complex critical to the maintenance of telomere length in most cancer cells (*4*). More recently, quadruplex-binding ligands have been shown to inhibit the activity of human telomerase (*5*). Since cancer cells typically exhibit substantial levels of telomerase, while normal somatic cells do not (*6*), a new modality of cancer chemotherapy has emerged based on stabilizing the folded quadruplex form of the 3′ overhang in the human telomere (*7*, *8*).

Targeting the quadruplex formed by the human telomere repeat, HT,[1] via structure-based methods requires knowledge of its detailed three-dimensional structure. Thus a series of efforts has been launched by a variety of groups to obtain high resolution structural information on this critically important species. An NMR study in the presence of Na^+ yielded a high resolution solution structure for the quadruplex formed by $d(AG_3(T_2AG_3)_3)$, based on an antiparallel folding pattern with a diagonal central loop, two lateral loops, and regular alternation of dG nucleosides between the *anti* and *syn* conformations (*9*), illustrated in Figure 1a. This structure served as an important model for the human telomere quadruplex, but due to the presence of higher intracellular concentrations of K^+ than Na^+ ions, there has been interest in obtaining the structure of this quadruplex in the presence of the former ion.

The first report of a high resolution structure for the HT quadruplex stabilized by K^+ entailed an X-ray crystal structure obtained in the presence of a quadruplex-binding ligand (*10*). The resulting structure was somewhat unusual as it involved a unimolecular parallel folding topology with three double-chain-reversal, or propeller, loops and all nucleosides in the *anti* conformation about the glycosidic bond (see Figure 1b). This high resolution crystal structure was dramatically different from that obtained in solution by NMR and led to multiple studies exploring other techniques to obtain evidence for a parallel folding conformation for this sequence when stabilized by K^+, some of which were confirmatory while others failed to find such evidence (*11*−*13*).

Very recently, several important studies have appeared aimed at solving the problem of conformational heterogeneity exhibited by the HT repeat quadruplex in solutions containing near-physiological concentrations of K^+ (100 mM). In one approach, Xu et al. used selective substitution of dG residues in $d(AG_3(T_2AG_3)_3)$ with ^{br}dG, in an effort to lock or freeze nucleosides into the *syn* conformation via bromination at the 8 position of guanine (*14*). Using CD spectra and melting curves, along with a judicious choice of substitutions, Xu et al. (*14*) identified two very stable conformations which they

† This work has been supported by NIH Grant GM067607.

* To whom correspondence should be addressed. Tel: 415-476-2761. Fax: 415-476-0688. E-mail: shafer@cgl.ucsf.edu.

[1] Abbreviations: TBA, thrombin binding aptamer; HT, human telomere sequence; PAGE, polyacrylamide gel electrophoresis.

10.1021/bi602392u CCC: $37.00
Published on Web 06/01/2007

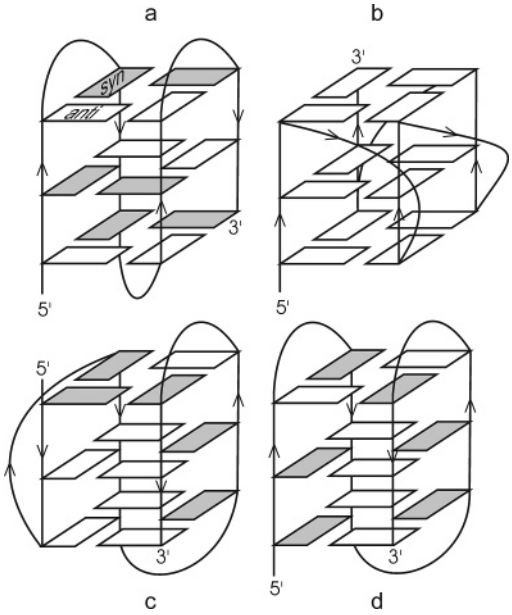

FIGURE 1: Different conformers for the human telomere sequence, d[$AG_3(T_2AG_3)_3$]. NMR solution structure in the presence of Na^+ (*9*), a; X-ray crystal structure in the presence of K^+ (*10*), b; mixed parallel−antiparallel (mixed-loop) structure in KCl solution determined by NMR (*17*, *18*), c; proposed alternate structure when stabilized by K^+ (*14*), d. Clear rectangles represent *anti* guanine nucleosides and shaded rectangles represent *syn* guanine nucleosides.

proposed were present together in solutions of the unmodified HT sequence, illustrated in Figure 1c,d. One structure involved an unusual hybrid or mixed folding topology consisting of three mutually parallel stretches of guanine and one antiparallel to the other three (see Figure 1c). Such a folding motif occurs via three lateral loops, one of which being a double-chain-reversal loop; in this case, this unusual loop conformation occurs in the first loop (starting from the 5′ end). While such loops are indeed unusual, other examples of quadruplexes have appeared containing such loops, e.g., the $d(T_2G_4)_4$ quadruplex formed in the presence of Na^+ (*15*) and the quadruplex formed by guanine-rich sequences in the BCL-2 promoter region (*16*). In these two latter cases, the double-chain-reversal loop is the last of the three loops in the structure. Thus the mixed parallel/antiparallel quadruplex formed by $d(AG_3(T_2AG_3)_3)$ when stabilized by K^+ ions appears unique in its configuration of loops.

Concomitant with the unusual array of loops, there is also an unusual alternation of *syn* and *anti* conformations, such that there are more dG's in the *anti* than *syn* conformation in the mixed parallel/antiparallel conformation, whereas in the strict antiparallel folding topologies, they appear in equal numbers. This may have important consequences for the CD spectrum of such species, as the all-parallel quadruplexes exhibit a major positive CD peak near 265 nm, while the classical antiparallel quadruplexes exhibit a major positive CD peak near 295 nm. Indeed, the CD spectrum of the BCL-2 promoter region quadruplex displays peaks at both 265 and 295 nm (*16*).

Two NMR papers appeared almost at the same time, addressing the problem of conformational heterogeneity observed in $d(AG_3(T_2AG_3)_3)$ in the presence of ~100 mM K^+ by adding some additional, mutant bases at each end of the sequence (*17*, *18*). In each case, the solution structures

Table 1: Oligodeoxyribo/Ribonucleotides Used in This Study

designation	sequence[a] (in 5′ to 3′ direction)
HT	AGGGTTAGGGTTAGGGTTAGGG
rHT1	aggguuaggguuaggguuaggg
rHT2	AgggTTAgggTTAgggTTAggg
rHT3	AgggTTAgggTTAGGGTTAGGG
rHT4	AgggTTAGGGTTAGGGTTAGGG
rHT5	AGggTTAGggTTAGGgTTAGgg
rHT6	AGGgTTAGggTTAGGgTTAGgg

[a] Ribonucleosides appear in lowercase.

contained the same folding topology as that described above, i.e., mixed parallel and antiparallel stretches of guanine connected first by a double-chain-reversal loop, followed by two lateral loops, with 7 *anti* dG's and 5 *syn* dG's.

In addition to this mixed parallel/antiparallel quadruplex conformation, the paper by Xu et al. (*14*) also proposed a model for the second conformation in the mixture formed by HT in KCl solution, illustrated in Figure 1d. This structure exhibits a more classical antiparallel folding topology involving three lateral loops, and we recently proposed such a structure for the K^+-stabilized quadruplex based on covalent ligation studies (*12*). Note that this conformation entails a less common *syn-syn-anti*/*syn-anti-anti* alternation within the stretches of guanine, which we and others have observed earlier for a dimeric hairpin quadruplex containing three quartets (*19*, *20*).

Here we approach the problems of refolding the human telomere quadruplex and of isolating and identifying individual conformers of the HT quadruplex in the presence of physiological concentrations of K^+ (140 mM) by selective substitution of deoxyguanosine nucleosides with riboguanosines, based on the preference for riboguanosines to adopt the *anti* conformation when incorporated into oligonucleotides (*21*). We have applied this method to engineer the refolding of the quadruplex formed by the thrombin binding aptamer (TBA), a 15-mer with the sequence $d(G_2T_2G_2TGTG_2T_2G_2)$ (*22*). The resulting parallel quadruplexes all formed bimolecular structures. In the case of the HT sequence, $d(AG_3(T_2AG_3)_3)$, we show here that both unimolecular and bimolecular parallel quadruplexes can be formed, depending on the extent of substitution. Furthermore, selective substitution of dG with rG suffices to isolate the mixed parallel−antiparallel stranded HT quadruplex described above.

MATERIALS AND METHODS

Oligonucleotides. All oligonucleotides (see Table 1) were obtained from IDT (Coralville, IA), with RNA and DNA/RNA chimeric sequences purified by RNase-free HPLC. Oligonucleotide concentrations were determined by UV spectrophotometry (Cary 100, Varian, Palo Alto, CA) using calculated extinction coefficients (*23*). Oligonucleotides were resuspended in 10 mM tris-acetate buffer, pH 6.7, and heated to 90 °C for 3 min, then cooled to room temperature prior to spectroscopic measurements.

Spectroscopy. UV spectra and melting curves were measured on a Cary 100 UV−visible spectrophotometer equipped with programmable Peltier heating. Thermal denaturation was carried out at a heating/cooling rate of 0.5 °C/min, with very little or no hysteresis. CD spectra were measured on an OLIS DMS10 spectrometer equipped with Peltier temperature control. 1D NMR spectra were measured in H_2O/D_2O (90%/10%) using a jump and return sequence for solvent suppression. Strand concentration was 0.22 mM; the solution contained 10 mM deuterated tris-acetate (pH 6.7), 100 μM TSP, and 140 mM KCl.

Polyacrylamide Gel Electrophoresis (PAGE). Polyacrylamide gels (20%, acrylamide/polyacrylamide, 19/1) were cast in 45 mM tris-acetate, which was also used for the gel buffer. Sequences were diluted to a final concentration of 40 μM, heated to 90 °C, and slowly cooled to room temperature in tris-acetate buffer (10 mM, pH 6.7) in the presence of 140 mM KCl. They were subjected to PAGE at 10 V/cm, 4 °C, stained with Stains-All, destained, and scanned into a computer.

Equilibrium Sedimentation. Oligonucleotide samples were analyzed by equilibrium sedimentation in a Beckman XL-A analytical ultracentrifuge in 10 mM tris-acetate buffer, pH 6.7, containing 140 mM KCl. Samples were dialyzed against the same buffer, and the dialysate was used in the reference cell. Oligonucleotides were run at 1 μM concentrations, and centrifugation was carried out over a period of several days, at 27,000 rpm and 20 °C. Molecular weights, *M*, were determined by calculating the slope of a semilog plot of the ratio of absorbances at 260 nm at a distance *r* from the center of rotation, $A(r)$, and at a reference distance r_o, $A(r_o)$, as a function of r^2, according to the formula

$$\ln \frac{A(r)}{A(r_o)} = \frac{\omega^2 M(1 - \bar{v}\rho)(r^2 - r_o^2)}{2RT}$$

where ω is the angular velocity, $\bar{v}$ is the partial specific volume of the DNA, ρ is the solution density, *R* is the gas constant, and *T* is the absolute temperature. For these calculations we assumed $\bar{v} = 0.55$ and $\rho = 1$. Calculated values for molecular weights were determined for the deprotonated oligonucleotide containing three specifically bound potassium ions.

RESULTS

The work we describe is presented here in two parts. First, we discuss the conformational behavior of HT, $d(AG_3(T_2AG_3)_3)$, and the DNA/RNA chimeric oligonucleotides rHT1, rHT2, rHT3, and rHT4 (Table 1), which were designed to change the folding motif of HT. Second, we examine the effect of rHT5 and rHT6 (Table 1), chimeric oligonucleotides designed to isolate single conformers corresponding to the mixture of conformers observed for HT in the presence of KCl.

Quadruplex Refolding. Our initial set of substitutions in $d(AG_3(T_2AG)_3)$ (HT) consisted of replacing all nucleosides with ribonucleosides (rHT1), all four runs of dG with rG (rHT2), the first two runs of dG with rG (rHT3), and the first run of dG with rG (rHT4), as detailed in Table 1. Based on our previous experience substituting ribonucleosides for deoxyribonucleosides, we anticipated that rHT1, the all-RNA analogue of HT, would form a parallel quadruplex, due to the strong preference of ribonucleosides for the *anti* conformation about the glycosidic bond. This is confirmed by the CD spectrum of rHT1, shown in Figure 2a, which exhibits the 265 nm positive peak characteristic of parallel quadruplexes. Also shown in Figure 2a is the CD spectrum of HT, with its principal peak at 295 nm, characteristic of antiparallel quadruplexes, and a very small shoulder near 270 nm.

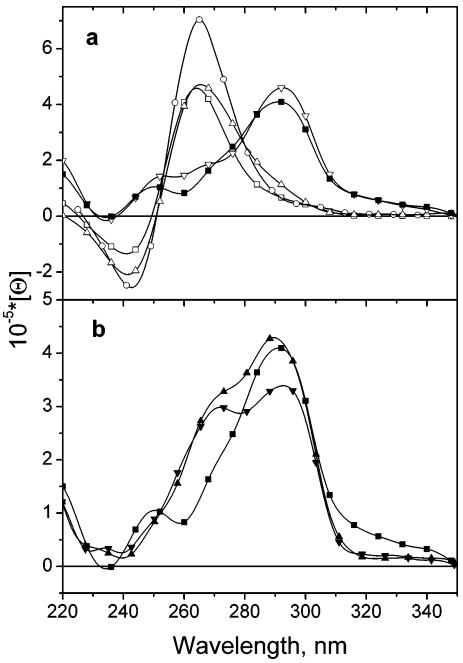

FIGURE 2: Molar ellipticity of sequences in 10 mM tris-acetate buffer, pH 6.7 in the presence of 140 mM KCl, measured at concentrations of 4−6 μM. (a) rHT1 (□), rHT2 (○), rHT3 (△), rHT4 (▽), and HT (■); (b) rHT5 (▲), rHT6 (▼), and HT (■).

We then reduced the extent of rG substitution from all nucleosides to, first, all guanine nucleosides (rHT2), then to half the guanine nucleosides (rHT3), and finally to a single stretch of 3 guanine nucleosides (rHT4). CD spectra for these three species are also presented in Figure 2a, where it can be seen that rHT2 and rHT3 both exhibit CD spectra characteristic of parallel quadruplexes. However, rHT4, with a single run of rG, shows a CD spectrum characteristic of antiparallel quadruplexes.

Having assessed the CD properties of these modified HT sequences, we then examined their gel electrophoretic mobility in an effort to obtain information concerning the number of strands composing these quadruplex structures. The results are shown in Figure 3a, where it can be seen that rHT1 migrates considerably more slowly than HT while rHT4 migrates at a rate very close to that of HT. The band for HT exhibits a mobility close to that for an unstructured 10-mer, indicative of a compact species consisting of a single, folded strand. In contrast, the significantly slower migration rHT1 suggests the presence of two or more strands.

The results in Figure 3a for the other two partially substituted sequences are more ambiguous, as their bands fall between those for HT4 and rHT1, with rHT2 closer to rHT1 and rHT3 closer to rHT4. In order to resolve this ambiguity, we subjected all four of these sequences, along with HT, to equilibrium centrifugation analysis. Results from these experiments are presented in Figure 4, where it can be

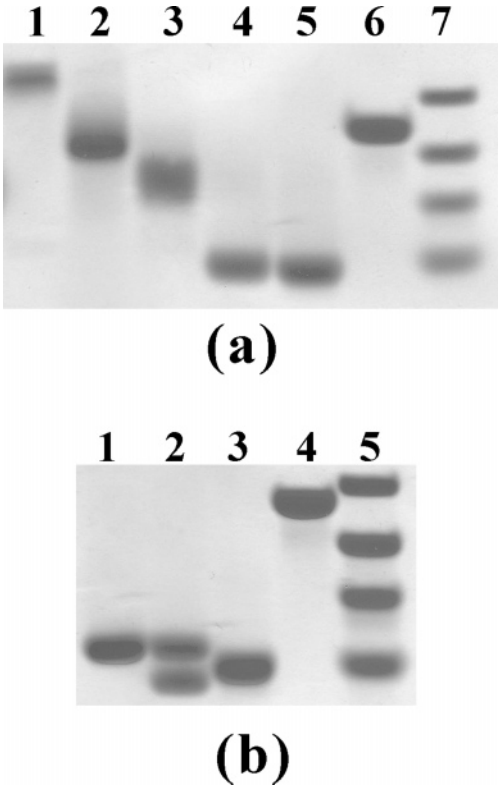

FIGURE 3: Native gel analysis of sequences in tris-acetate (10 mM, pH 6.7) in the presence of 140 mM KCl. **(**a**)** Lanes 1 to 5: rHT1, rHT2, rHT3, rHT4, and HT, respectively. Lane 6: U_{20}. Lane 7: DNA ladder ($d(T_{27})$, $d(T_{20})$, $d(T_{15})$, and $d(T_{10})$). **(**b**)** Lanes 1 to 3: rHT5, rHT6, and HT, respectively. Lane 4: U_{20}. Lane 5: DNA ladder ($d(T_{27})$, $d(T_{20})$, $d(T_{15})$, and $d(T_{10})$).

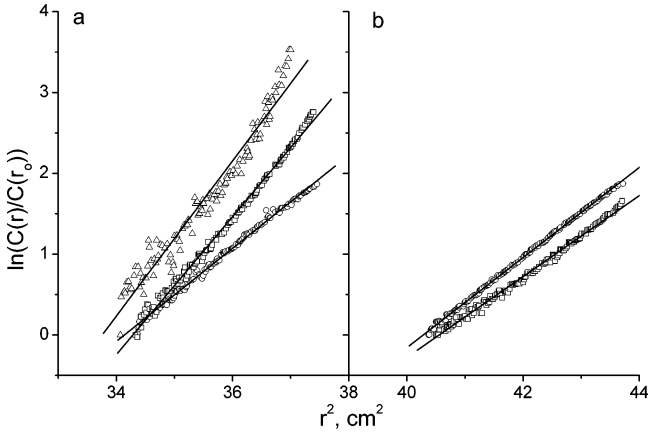

FIGURE 4: Equilibrium sedimentation results measured in 10 mM tris-acetate buffer, pH 6.7, 140 mM KCl at 20 °C for (a) rHT1 (□), rHT2 (△), rHT4 (○); (b) rHT3 (□), HT (○).

seen that most plots are quite linear, although some show signs of curvature, due to RNA degradation, as evidenced by gels run postcentrifugation (data not shown). As expected, this behavior was not observed with the all-DNA HT sequence. The presence of some degradation products results in an observed weight average molecular weight that is smaller than predicted for intact structures, but still permits discerning whether these sequences form unimolecular or bimolecular species. The resulting molecular weights are presented in Table 2, where it can be seen that HT, rHT3, and rHT4 sediment as single strands, while rHT1 and rHT2 both appear to sediment as double-stranded structures.

Table 2: Molecular Weights Determined from Equilibrium Sedimentation Experiments

	molecular weight (Da)	
sequence	exptl	calcd
HT	7600	7063
rHT1	11600	7415
rHT2	13100	7255
rHT3	6827	7159
rHT4	7860	7111

Table 3: Thermodynamic Parameters from UV Melting Analysis for Unimolecular Quadruplex Dissociation in 10 mM Tris-acetate, pH 6.7, and 140 mM KCl

sequence	T_m (°C)[a]	ΔH (kcal/mol)[b]	ΔS (cal/mol-K)[b]	ΔG(25 °C) (kcal/mol)[b]
HT	70.5	49.4	144	6.54
rHT3	63.6	40.6	121	4.66
rHT4	63.3	40.8	121	4.65
rHT5	75.3	69.1	198	9.99
rHT6	75.7	64.3	184	9.35

[a] Experimental error estimated at ±0.5 °C. [b] Experimental error estimated at ±10%.

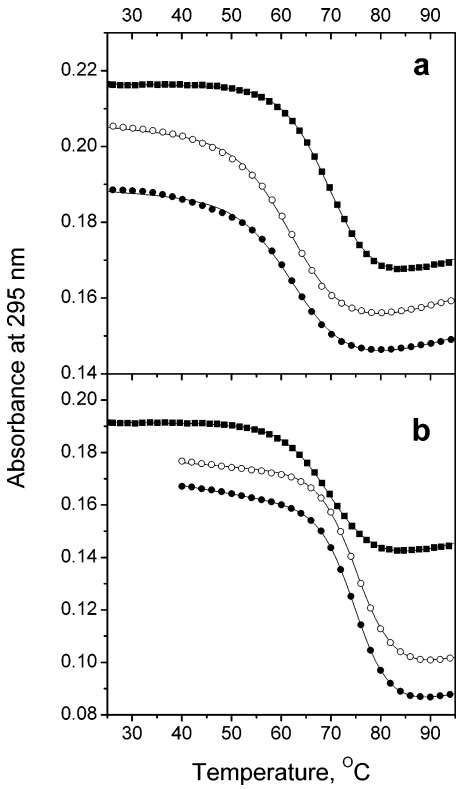

FIGURE 5: Melting curves of unimolecular quadruplexes (~5 μM) in 10 mM tris-acetate buffer, pH 6.7, in the presence of 140 mM KCl. (a) rHT3 (●), rHT4 (○), and HT (■). (b) rHT5 (●), rHT6 (○), and HT (■) (displaced on vertical scale for clarity).

Thermodynamic stability of the unimolecular species rHT3 and rHT4 was assessed by UV melting curves (see Figure 5a), which were analyzed according to a two-state model for quadruplex unfolding, accompanied by $\Delta C_P = 0$. Results from this analysis are presented in Table 3. Interestingly, rHT3 and rHT4 have almost identical thermodynamic parameters and stability, despite the fact that the former exhibits a parallel fold while the latter exhibits an antiparallel fold. These two sequences differ in that rHT3 has three more

rG nucleosides than rHT4, which suffices to refold the quadruplex, maintaining single-strand stoichiometry. Included in both Figure 5a and Table 3 are results for HT for comparison purposes. While the HT melting curve exhibits a single transition, NMR results indicate that HT exists as a mixture of least two species in KCl (*17*, *18*). Thus quantitative analysis of melting curves may represent some kind of average result for these species. That they have similar thermal stabilities is apparent in the appearance of a single transition in the melting curve for HT. Nonetheless, it is clear that both rHT3 and rHT4 are significantly less stable than HT, in terms of both melting temperature and enthalpy changes, although more stable in terms of a smaller entropy decrease accompanying quadruplex formation.

At this point, it is difficult to determine whether differences in the enthalpy and entropy changes observed for these two chimeric sequences, relative to HT, derive from stacking, loop effects, or other interactions. In terms of the effect of substituting rG for dG, there is evidence that little difference exists in preferences for *syn*/*anti* conformations between purine nucleosides (*21*), although significant differences are seen when nucleosides are incorporated into larger secondary structural units. Thus these differences in *syn*/*anti* conformations are only manifested in the context of more complicated structures and likely involve differences in stacking etc. resulting from the overall structure. Sugar pucker differences between rG and dG may also play a role. Another difference between dG and rG is the presence of an additional hydrogen-bonding group, the 2′-OH on the latter. While this may also contribute to differences in stability, there is little evidence at this time that it would contribute to differences in folding patterns. The observation that both rHT3 and rHT4 exhibit reduced stability compared to HT suggests that the folds they exhibit are different and inherently less stable than those of HT.

Conformer Selection. We next investigated sequences having more site-specific substitutions of rG for dG. In particular, we explored the possibility of isolating a single quadruplex conformation from the mixture reported for HT stabilized by K^+ (*17*, *18*). The recent CD and NMR studies on HT and modified HT sequences all agree on the folding pattern for one of the structures, the mixed parallel/antiparallel quadruplex structure illustrated schematically in Figure 1c. In an effort to select out this particular conformation, we investigated rHT5, containing rG at all the *anti* positions reported for the mixed parallel/antiparallel structure. The rationale was to exploit the preference of rG for the *anti* conformation in order to stabilize the mixed-loop conformation (Figure 1c) relative to the alternative conformation (Figure 1d). Similarly, we also investigated rHT6 as a possible approach to isolating this alternative conformation.

CD spectra for these sequences are shown in Figure 2b, where it can be seen that rHT5 possesses a main band at 295 nm along with a significant shoulder near 270 nm, similar to what has been reported for the mixed-loop structure determined by Ambrus et al. (*17*). In contrast, the CD spectrum for rHT6 shows a more pronounced peak near 270, possibly indicating the presence of more than one species.

Again, as CD spectra cannot readily distinguish between a single conformation and a mixture of conformations, we subjected these sequences to native gel electrophoresis, the results of which are presented in Figure 3b. Here it is readily apparent that rHT5 runs as a single band while rHT6 exhibits two bands, confirming the presence of a second species in the latter sample. In order to assess the effects of these substitutions on the thermal stability of the resulting unimolecular quadruplex structures, we carried out UV melting studies on these sequences as well, and, as can be seen in Figure 5b and Table 3, the substitutions leading to rHT5 and rHT6 led to significantly greater stability than the parent sequence, HT, and the other sequences, although not as great an enhancement as seen by Xu et al. (*14*) for the multiply brominated sequences. That large effect is related to the fact that bromination of dG at the 8 position substantially changes the *syn*/*anti* equilibrium even at the nucleoside level. The enthalpy changes associated with rHT5 and rHT6 are substantially greater than those of HT, by almost 20 kcal/mol for rHT5. This relatively large effect may be due to stacking differences between HT and the chimeric sequences, which are presumably in the same fold(s) as those exhibited by HT, in contrast to rHT3 and rHT4, which most likely possess different folds. This could arise from differences in the sugar pucker, for example, affecting the resulting stacking interactions. As in the case of HT, the results for HT6, which consists of two species with apparently very similar T_ms, represent an average for those species.

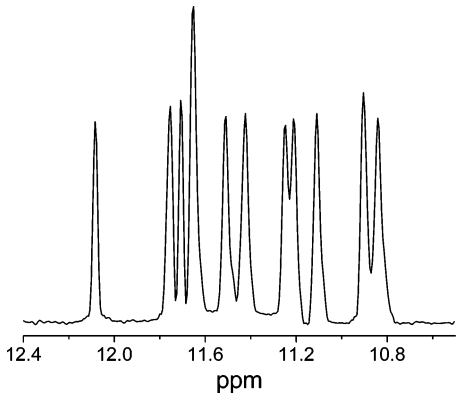

FIGURE 6: Imino proton NMR spectrum of HT5 at 0.165 mM strand concentration measured in 10 mM tris-acetate, pH 6.7, 140 mM KCl at 25 °C.

We next examined the imino proton NMR spectrum of rHT5, shown in Figure 6. This spectrum shows 11 well-resolved imino proton peaks, with one likely corresponding to two protons, as expected for a stable quadruplex consisting of three guanine quartets. Additionally, there is little or no sign of peaks from a minor species, confirming the gel electrophoresis result that rHT5 migrates as a single species. We note that these peaks appear in the same frequency range as those observed for the recently reported HT analogues containing flanking bases (*17*, *18*). When an equal amount of NaCl is added to this sample, its imino proton spectrum remains unchanged (data not shown).

DISCUSSION

In a previous publication (*22*), we reported our initial results showing that selective substitution of deoxyriboguanosine by riboguanosine can refold the quadruplex formed by the thrombin binding aptamer, TBA, from an antiparallel fold to a parallel fold, and vice versa. This approach to

quadruplex refolding is based on the strong preference for the *anti* conformation about the glycoside bond observed for riboguanosine when incorporated into oligo- and polynucleotides. Thus, at sequence positions containing a *syn* dG in an antiparallel quadruplex, replacement with rG drives the nucleosides at those positions to maintain the *anti* conformation, resulting in a parallel conformation. As expected, the fully RNA analogue of TBA also folds into a parallel quadruplex. At appropriate positions, replacement of rG in the all-RNA version of TBA with dG leads to an antiparallel fold.

Several other observations arose in that study on TBA. All of the parallel folding sequences appeared to form dimeric or two-stranded quadruplexes, while all the antiparallel quadruplexes were unimolecular. This somewhat unexpected result indicated the possibility that parallel unimolecular quadruplexes consisting of two quartets are energetically unfeasible. Studies on additional RNA-containing sequences based on TBA provide additional support for this conclusion, in that no evidence for a unimolecular, parallel two-quartet quadruplex was obtained (data not shown). A parallel folded quadruplex has been reported for $d(GGA)_4$ containing one quartet and one heptad consisting of GAGAGAG bases (*24*). The additional stacking and hydrogen-bonding interactions in the heptad apparently stabilize the parallel fold in this case.

In the results presented above, we first demonstrate that similar substitution of rG for dG in HT can lead to quadruplex refolding, resulting in parallel quadruplexes, based on major changes in CD spectra. The interpretation of CD spectra in terms of the overall quadruplex folding topology has proved to be quite reliable in general, although some have suggested that it may not always lead to the correct result (*25*). Nonetheless, the vast majority of published reports are consistent with the observation of a major positive band at 265 nm for parallel quadruplexes (all *anti* nucleosides) and at 295 nm for antiparallel quadruplexes (mixture of *syn* and *anti* nucleosides). This has been shown to be the case for the linear, tetramolecular quadruplex $[d(TGGGGT)]_4$ (*26*, *27*); Lu et al. first reported evidence supporting this observation in folded quadruplexes by constructing a sequence constrained to form a parallel, dimeric quadruplex via an unusual 5′−5′ linkage (*28*). More recently, Virgilio et al. have provided additional evidence relating CD spectra to glycosidic bond conformation by examining modifications of the sequence d(TGGGT) in which a single G is replaced by ^{me}G, 8-methyl guanine (*29*). Methylation at this position is known to favor the *syn* conformation (*30*). Using high resolution NMR and CD spectroscopies, they observed that quadruplex structures exhibiting the 265 nm CD peak—$d(TGGGT)_4$ and $d(TG^{me}GGT)_4$—were characterized by all nucleosides in the *anti* conformation, even the methylated ones. In contrast, $d(T^{me}GGGT)_4$ exhibited a 295 nm peak and its methylated nucleosides were in the *syn* conformation, with the remaining nucleosides in the *anti* conformation. Thus the position of the CD signal is really determined by the presence or absence of *syn* nucleosides rather than strand alignment. A CD peak at 265 nm, then, implies an all-*anti* arrangement, which can only be realized by an all-parallel strand alignment.

There are several other examples of high resolution structures that follow this pattern. The sequence $d(GGA)_4$ was shown by NMR to form a parallel-folded quadruplex structure and by CD to exhibit a band at 265 nm (*24*). A guanine-rich sequence from the *c-myc* promoter has been shown by NMR to fold into a unimolecular, parallel quadruplex (*31*) with a CD band a 265 nm (*32*). Similarly, a parallel, bimolecular quadruplex which inhibits HIV integrase has been shown by NMR to form a parallel fold, with a CD band near 265 nm (*33*). The one exception to these observations is the sequence T30695, which possesses a CD band near 265 nm (*34*) yet has been described as forming an antiparallel quadruplex as determined by NMR analysis (*35*). However, doubts concerning the proposed antiparallel structure for T30695 have been raised by both Patel and co-workers (*33*) and Hurley and co-workers (*32*), based on work carried out on closely related sequences. Thus, we are quite confident that the very distinct spectra described above can be used to distinguish parallel from antiparallel quadruplex conformations.

Table 4: Summary of Folding Pattern and Molecularity of Quadruplex Structures Formed in 140 mM KCl

sequence	no. of strands	folding pattern
HT	1	mixture of conformers, one of which exhibits mixed parallel−antiparallel pattern
rHT1	2	parallel
rHT2	2	parallel
rHT3	1	parallel
rHT4	1	antiparallel
rHT5	1	mixed parallel−antiparallel
rHT6	1	mixture of conformers

In contrast to our previous results on TBA (*22*), it is possible to obtain both dimeric and monomeric parallel quadruplex forms for HT. Table 4 summarizes the molecularity and folding pattern for each of the chimeric oligonucleotides examined. HT3, for example, is parallel and unimolecular, indicating that substitution of half the dG residues suffices to completely refold the quadruplex while maintaining single-stranded stoichiometry. It is possible that this particular sequence realizes in solution the same parallel, unimolecular conformation observed by X-ray crystallography (*10*). In the case of rHT4, which exhibits an antiparallel folding motif, a single stretch of rG's does not suffice to refold the quadruplex. In the case of rHT1 and rHT2, a parallel quadruplex conformation is observed but the structure consists of two strands. It is not clear at this point why these two latter sequences do not fold unimolecularly.

Due to the potential importance of the human telomere quadruplex as a target for cancer chemotherapy, there is much interest in determining its structure in order to facilitate structure-based drug design. The three recent studies (*14*, *17*, *18*) on HT sequences have come, perhaps, closest to assessing a biologically relevant solution structure for this quadruplex. And in each case, some form of modification of the sequence was necessary in order to isolate a single species from the two principal conformations that are observed for the unmodified HT sequence when stabilized by K^+. The necessity for modifications raises the question of the extent to which the resulting isolated conformation resembles that of one of the unmodified sequences. Here

we provide an alternative approach to modification that also leads to a single conformer under these solution conditions.

Another observation made in our earlier work on chimeric substitutions in TBA is that, among the antiparallel quadruplexes formed, those containing rG nucleosides in the *anti* positions of the all-DNA aptamer possessed a greater thermal stability than the all-DNA sequence itself. Thus the strong tendency for rG to maintain the *anti* conformation led to increased stability in those cases. We anticipated that a similar set of substitutions in HT matching the *anti* positions of the mixed parallel−antiparallel conformation would enhance the stability of that particular conformer, possibly leading to low or undetectable amounts of the alternate conformation. In the results described above, we demonstrate the validity of this approach by showing that rHT5 exists as a single species with great stability than HT, consistent with stabilization of the mixed parallel−antiparallel conformation reported recently (*14*, *17*, *18*). This result is also in agreement with the two structures proposed by Xu et al. (*14*), shown in Figure 1c,d, where the only sugar that exhibits a different conformation about the glycosidic bond between the two structures is G3, which is a ribonucleoside in rHT5. In order for rHT5 to convert from the mixed-loop to the all-lateral-loop antiparallel conformation, this nucleoside would have to change from the *anti* to the *syn* conformation, which is highly unfavored for ribonucleosides.

In contrast, there is little or no barrier to dG changing from the *syn* to the *anti* conformation, and hence we suggest that rHT6 exists as a mixture of the two conformations shown in Figure 1c,d. The gel results certainly indicate the presence of two, or at least two, conformers, but the CD spectra do not appear to be consistent with a linear combination of the spectra for rHT5 and for an all-lateral-loop antiparallel quadruplex, which would not be expected to show any peak or shoulder at 265−270 nm. This raises the possibility that the conformation giving rise to the extra band in the gel belongs to yet another folding motif. Additional studies will be needed to address this question.

In summary, we have shown that the quadruplex formed by the human telomere repeat sequence can be refolded from an antiparallel to a parallel topology via substitution of specific deoxyriboguanosines with riboguanosines. In certain cases, the resulting parallel quadruplex maintains its unimolecular configuration while in others it changes to a bimolecular configuration. Furthermore, this approach can also be used to select out a single conformation from a mixture, in particular individual conformations of HT stabilized by K^+, as has recently been done by other means. Selecting out single structures from a mixture has necessitated the use of HT sequences containing mutant terminal bases, selective bromination, or selective substitution of dG by rG. The extent to which any or all of these modifications perturb the actual solution structure of the resulting human telomere quadruplex conformer remains to be determined. The approach described here has been used to engineer the folding pattern of the thrombin binding aptamer quadruplex (*22*) and now the human telomere quadruplex, and thus is likely to serve as a general method for controlling quadruplex folding patterns.

ACKNOWLEDGMENT

It is a pleasure to acknowledge the help of Professor Peter Walter and Drs. Pascal Egea and Joel Credle, Department of Biochemistry and Biophysics, UCSF, for help in carrying out the sedimentation experiments, of Dr. Zhihua Du, Department of Pharmaceutical Chemistry, UCSF, for assistance with NMR spectra, and Ms. Susannah Yu for help in carrying out some CD and gel experiments.

REFERENCES

1. Blackburn, E. H. (1991) *Nature 350*, 569−573.
2. Haider, S., Parkinson, G. N., and Neidle, S. (2002) *J. Mol. Biol. 320*, 189−200.
3. Smirnov, I. V., Kotch, F. W., Pickering, I. J., Davis, J. T., and Shafer, R. H. (2002) *Biochemistry 41*, 12133−12139.
4. Zahler, A. M., Williamson, J. R., Cech, T. R., and Prescott, D. M. (1991) *Nature 350*, 718−720.
5. Sun, D. Y., Thompson, B., Cathers, B. E., Salazar, M., Kerwin, S. M., Trent, J. O., Jenkins, T. C., Neidle, S., and Hurley, L. H. (1997) *J. Med. Chem. 40*, 2113−2116.
6. Kim, N. W., Piatyszek, M. A., Prowse, K. R., Harley, C. B., West, M. D., Ho, P. L., Coviello, G. M., Wright, W. E., Weinrich, S. L., and Shay, J. W. (1994) *Science 266*, 2011−2015.
7. Read, M., Harrison, R. J., Romagnoli, B., Tanious, F. A., Gowan, S. H., Reszka, A. P., Wilson, W. D., Kelland, L. R., and Neidle, S. (2001) *Proc. Natl. Acad. Sci. U.S.A. 98*, 4844−4849.
8. Han, H., and Hurley, L. H. (2000) *Trends Pharmacol. Sci. 21*, 136−142.
9. Wang, Y., and Patel, D. J. (1993) *Structure 1* 263−282.
10. Parkinson, G. N., Lee, M. P., and Neidle, S. (2002) *Nature 417*, 876−880.
11. Ourliac-Garnier, I., Elizondo-Riojas, M. A., Redon, S., Farrell, N. P., and Bombard, S. (2005) *Biochemistry 44*, 10620−10634.
12. Qi, J., and Shafer, R. H. (2005) *Nucleic Acids Res. 33*, 3185−3192.
13. Li, J., Correia, J. J., Wang, L., Trent, J. O., and Chaires, J. B. (2005) *Nucleic Acids Res. 33*, 4649−4659.
14. Xu, Y., Noguchi, Y., and Sugiyama, H. (2006) *Bioorg. Med. Chem. 14*, 5584−5591.
15. Wang, Y., and Patel, D. J. (1994) *Structure 2*, 1141−1156.
16. Dai, J., Dexheimer, T. S., Chen, D., Carver, M., Ambrus, A., Jones, R. A., and Yang, D. (2006) *J. Am. Chem. Soc. 128*, 1096−1098.
17. Ambrus, A., Chen, D., Dai, J., Bialis, T., Jones, R. A., and Yang, D. (2006) *Nucleic Acids Res. 34*, 2723−2735.
18. Luu, K. N., Phan, A. T., Kuryavyi, V., Lacroix, L., and Patel, D. J. (2006) *J. Am. Chem. Soc. 128*, 9963−9970.
19. Strahan, G. D., Shafer, R. H., and Keniry, M. A. (1994) *Nucleic Acids Res. 22*, 5447−5455.
20. Smith, F. W., Lau, F. W., and Feigon, J. (1994) *Proc. Natl. Acad. Sci. U.S.A. 91*, 10546−10550.
21. Saenger, W. (1984) *Principles of Nucleic Acid Structure*, Springer-Verlag, Berlin.
22. Tang, C. F., and Shafer, R. H. (2006) *J. Am. Chem. Soc. 128*, 5966−5973.
23. Gray, D. M., Hung, S. H., and Johnson, K. H. (1995) *Methods Enzymol. 246*, 19−34.
24. Matsugami, A., Ouhashi, K., Kanagawa, M., Liu, H., Kanagawa, S., Uesugi, S., and Katahira, M. (2001) *J. Mol. Biol. 313*, 255−269.
25. Hazel, P., Huppert, J., Balasubramanian, S., and Neidle, S. (2004) *J. Am. Chem. Soc. 126*, 16405−16415.
26. Petraccone, L., Erra, E., Duro, I., Esposito, V., Randazzo, A., Mayol, L., Mattia, C. A., Barone, G., and Giancola, C. (2005) *Nucleosides Nucleotides Nucleic Acids 24*, 757−760.
27. Phillips, K., Dauter, Z., Murchie, A. I. H., Lilley, D. M. J., and Luisi, B. (1997) *J. Mol. Biol. 273*, 171−182.
28. Lu, M., Guo, Q., and Kallenbach, N. R. (1993) *Biochemistry 32*, 598−601.
29. Virgilio, A., Esposito, V., Randazzo, A., Mayol, L., and Galeone, A. (2005) *Nucleic Acids Res. 33*, 6188−6195.
30. Sugiyama, H., Kawai, K., Matsunaga, A., Fujimoto, K., Saito, I., Robinson, H., and Wang, A. H. (1996) *Nucleic Acids Res. 24*, 1272−1278.
31. Ambrus, A., Chen, D., Dai, J., Jones, R. A., and Yang, D. (2005) *Biochemistry 44*, 2048−2058.

32. Seenisamy, J., Rezler, E. M., Powell, T. J., Tye, D., Gokhale, V., Joshi, C. S., Siddiqui-Jain, A., and Hurley, L. H. (2004) *J. Am. Chem. Soc. 126*, 8702−8709.
33. Phan, A. T., Kuryavyi, V., Ma, J. B., Faure, A., Andreola, M. L., and Patel, D. J. (2005) *Proc. Natl. Acad. Sci. U.S.A. 102*, 634−639.
34. Jing, N., Rando, R. F., Pommier, Y., and Hogan, M. E. (1997) *Biochemistry 36*, 12498−12505.
35. Jing, N., and Hogan, M. E. (1998) *J. Biol. Chem. 273*, 34992−34999.

BI602392U